DOI: 10.1002/ejic.201100809

Control of the Coordination Geometry Around Platinum by a Supramolecular Capsule

Tehila S. Koblenz,[a] Henk L. Dekker,[b] Chris G. de Koster,[b] Piet W. N. M. van Leeuwen,[a] and Joost N. H. Reek*[a]

Keywords: Supramolecular chemistry / Supramolecular capsules / Platinum / Calixarenes / Ionic interactions / Phosphane ligands

The coordination geometry around a platinum atom can be controlled by a diphosphane capsule composed of a tetracationic xantphos-type ligand and a tetraanionic calix[4]arene. Reaction of the diphosphane capsule with the platinum precursor $[PtCl_2(MeCN)_2]$ yields the bisligated biscalix[4]arene *trans*-platinum capsule, whereas the same diphosphane in the absence of calix[4]arene prefers the formation of the monoligated *cis*-platinum complex, as indicated by $^{31}P\{^1H\}$ NMR and ESI-MS. The two calix[4]arenes stabilize the kinetic product (*trans*-Pt), and slow the formation of the thermodynamic product (*cis*-Pt).

Introduction

The catalytic properties of transition metal complexes depend on ligand parameters such as steric and electronic properties, bite angle and chirality. Supramolecular chemistry provides new strategies for influencing ligand parameters and consequently the properties of their transition metal complexes.[1] We have encapsulated transition metals by applying pyridylphosphane ligands, which coordinate the transition metal through the phosphorus atom, and at the same time, the nitrogen atoms of the pyridyl groups selectively coordinate to Zn^{II}–porphyrins or Zn^{II}–salphens, resulting in a hemispherical ligand–template capsule around the transition metal (Figure 1, a).[2] When tris(*m*-pyridyl)-phosphane is applied, the steric hindrance created around the metal results in the decoordination of one of the two pyridylphosphane ligands. These encapsulated rhodium complexes were shown to have unusual reactivity and selectivity in the hydroformylation of terminal and internal alkenes. Interestingly, the tris(*m*-pyridyl)phosphane and tris(*p*-pyridyl)phosphane give rise to very different complexes. For example, addition of 6 equiv. of Zn^{II}–salphen to *cis*-$[Pt(\mathbf{P_A})_2Cl_2]$ [$\mathbf{P_A}$ = tris(*p*-pyridyl)phosphane] did not lead to ligand dissociation but gave rise to the exclusive formation of the encapsulated *trans*-Pt complex *trans*-$[Pt\{(Zn)_3\cdot\mathbf{P_A}\}_2Cl_2]$.[2d] This *cis*-to-*trans* isomerism is induced by the second coordination sphere around the transition metal.

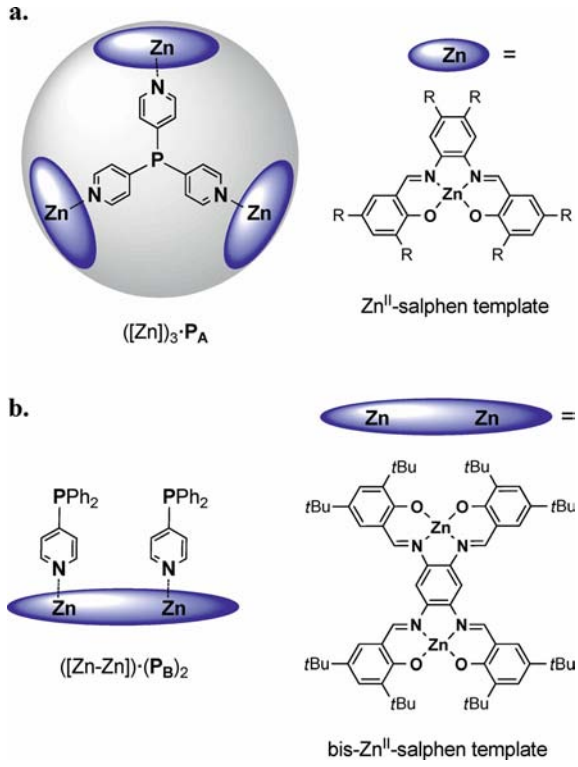

Figure 1. Hemispherical ligand–template capsule (a) and templated chelating bidentate ligand (b).

Chelating (hetero)bidentate ligands can be assembled from two monodentate ligands by equipping them with complementary binding motifs or by applying a template

[a] Homogeneous and Supramolecular Catalysis, Van't Hoff Institute for Molecular Sciences, University of Amsterdam, Postbox 94720, 1090 GS Amsterdam, The Netherlands
Fax: +31-20-5255604
E-mail: J.N.H.Reek@uva.nl
[b] Mass Spectrometry of Biomacromolecules, Swammerdam Institute for Life Sciences, University of Amsterdam, Postbox 94720, 1090 GS Amsterdam, The Netherlands
Supporting information for this article is available on the WWW under http://dx.doi.org/10.1002/ejic.201100809.

that contains two binding sites for the two monodentate ligands.[3] We have previously studied the template-induced formation of chelating bidentate ligands by the selective self-assembly of two monodentate pyridylphosphane ligands ($\mathbf{P_B}$) on a rigid biszinc(II) salphen template with two identical binding sites (Figure 1, b).[3b] Addition of the template to *cis*-[Pt($\mathbf{P_B}$)$_2$Cl$_2$] resulted in a mixture of the templated *cis*-Pt complex (15%) and templated *trans*-Pt complex (85%). The templated *trans*-Pt complex is the thermodynamic product and is stabilized by the formation of a bidentate chelating ligand.

We report here a supramolecular diphosphane capsule, which controls the coordination geometry around a platinum atom. Supramolecular capsules are composed of two or more, not necessarily identical, building blocks programmed to self-assemble in solution into the desired structure.[1b,1c,4] We have previously reported capsule **A·C**, which is formed by ionic interactions and composed of a tetracationic xantphos-type diphosphane **A** and the complementary tetraanionic calix[4]arene **C** (Scheme 1).[5] The free and bound building blocks of **A·C** undergo a fast exchange on the NMR time scale. Encapsulation of a transition metal within this framework is achieved by using the metal complex of the tetracationic diphosphane ligand for the assembly process. The encapsulated metal is still available for catalytic transformations as it is not involved in the assembly process.[5a–5b] We have recently demonstrated that encapsulation of a rhodium hydroformylation catalyst in this diphosphane-based capsule results in new product regioselectivities, high product chemoselectivity and substrate selectivity.[5d]

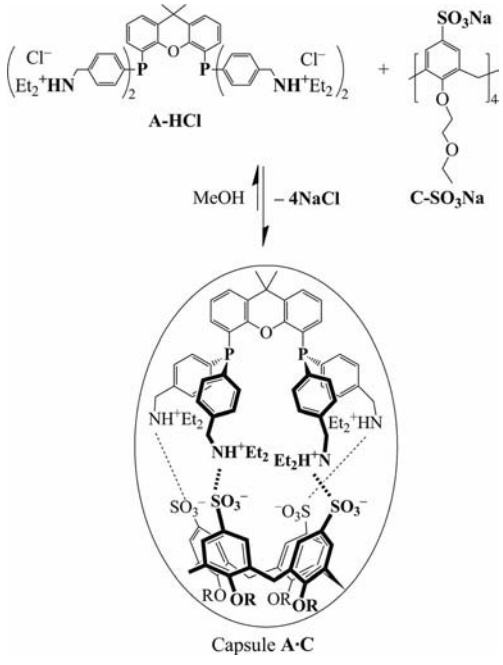

Scheme 1. Self-assembly of **A·C** composed of diphosphane **A** and calixarene **C**.

Xantphos ligands have large natural bite angles, typically between 100 and 120° (P–M–P angle), which can act as both a *cis* and *trans* chelating ligand in square planar palladium(II) and platinum(II) complexes, as shown by van Leeuwen and coworkers.[6] Kollar and coworkers have synthesized the *cis*-[Pt(xantphos)Cl$_2$] complex by heating [PtCl$_2$(PhCN)$_2$] and xantphos in a 1:1 ratio in benzene (Scheme 2).[7] Addition of a second equivalent of xantphos to the *cis*-Pt complex at room temperature resulted in a *cis*-to-*trans* rearrangement, to give the ionic *trans*-[Pt(xantphos)(η^1-xantphos)Cl]Cl complex with the second xantphos ligand coordinating in a monodentate fashion. The platinum–xantphos–tin(II) chloride system, which is a mixture of *cis*- and *trans* complexes, has been applied as a hydroformylation catalyst.[6h,7,8] Van Leeuwen and coworkers, Matt and coworkers and den Heeten have reported *trans*-[PtCl$_2$(diphosphane)] complexes using the *trans*-spanning diphosphane ligand SPANphos, *trans*-spanning diphosphanes based on a cyclodextrin cavity and a cyclic bisxantphos ligand, respectively.[9] To the best of our knowledge, a platinum dichloride complex containing only one *trans*-coordinating xantphos-type ligand, i.e. *trans*-[Pt(xantphos)Cl$_2$], has not been reported.

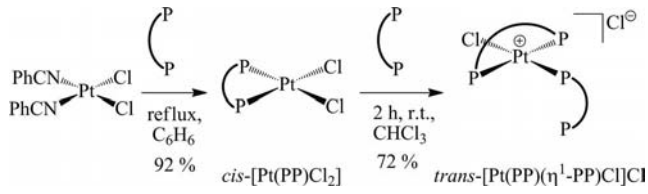

Scheme 2. Synthesis of *cis*- and *trans*-platinum(II) xantphos complexes.[7]

Results and Discussion

1. Platinum Complexes

We compared the reaction between the tetracationic xantphos-type ligand **A-HOTs** (**A**) and [PtCl$_2$(MeCN)$_2$] with the reaction between the diphosphane capsule **A·C** and [PtCl$_2$(MeCN)$_2$]. The products were characterized by ^{31}P{^{1}H} NMR spectroscopy and ESI-MS, see Exp. Sect. and Supporting Information. The molecular structure of **A-HOTs** (**A**) is given in Figure 2. Depending on the conditions used, the reaction of [PtCl$_2$(MeCN)$_2$] with **A** in methanol led to the formation of *cis*-[Pt(**A**)Cl$_2$] ($\mathbf{B_1}$) and/or *trans*-[Pt(**A**)(η^1-**A**)Cl]Cl ($\mathbf{B_2}$), vide infra, as indicated by in situ ^{31}P{^{1}H} NMR spectroscopy and ESI-MS (Scheme 3 and Table 2, Entries 1 and 3). The ^{31}P{^{1}H} NMR spectrum of *cis*-$\mathbf{B_1}$ shows a characteristic 1/4/1 pattern consisting of a singlet at 6.2 ppm, flanked by ^{195}Pt satellites with a coupling constant J_{Pt-P} of 3728 Hz (Table 1 and Figure 4, b). This coupling constant indicates that a chloride ligand is present *trans* to the phosphorus donor, in line with the *cis*-chelation of **A**.[7,8,10] The ^{31}P{^{1}H} NMR spectrum of *trans*-$\mathbf{B_2}$ shows the presence of three different phosphorus atoms

(Table 1, Figures 3 and 4, c): a triplet signal for P_X at 15.9 ppm (1 P) flanked by ^{195}Pt satellites with J_{Pt-P} of 4074 Hz, a doublet signal for P_Y at 15.0 ppm (2 P) flanked by ^{195}Pt satellites with J_{Pt-P} of 2679 Hz, indicating that the two phosphorus atoms are *trans* to one another, and a singlet signal at –22.6 ppm (1 P) assigned to P_Z, the noncoordinating phosphorus atom of the monodentate ligand.[7,10] The triplet and doublet signals have a *cis* coupling constant J_{P-P} of 18.1 Hz.

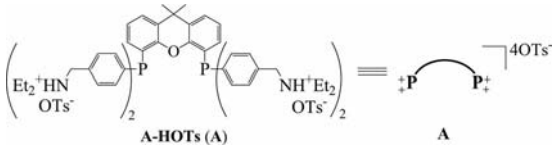

Figure 2. Molecular structure of **A**.

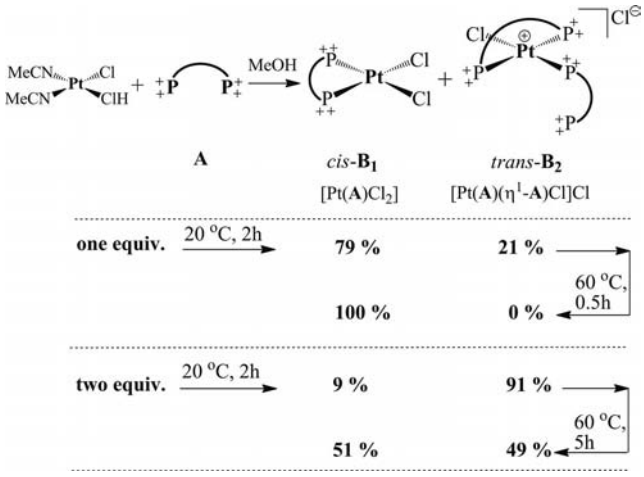

Scheme 3. Reaction of $[PtCl_2(MeCN)_2]$ with **A** to give *cis*-$\mathbf{B_1}$ and *trans*-$\mathbf{B_2}$.

Table 1. $^{31}P\{^1H\}$ NMR spectroscopic data of the diphosphanes, platinum complexes and capsules.[a]

	δP_X[b] [ppm]	δP_Y[b] [ppm]	δP_Z [ppm]	$^1J_{Pt-P_X}$ [Hz]	$^1J_{Pt-P_Y}$ [Hz]	$^2J_{P_X-P_Y}$ [Hz]
A	–16.9 (s)	–	–	–	–	–
A·**C**	–17.5 (s)	–	–	–	–	–
cis-$\mathbf{B_1}$	6.2 (s)	–	–	3728	–	–
(*cis*-$\mathbf{B_1}$)·**C**	6.6 (s)	–	–	3727	–	–
trans-$\mathbf{B_2}$	15.9 (t)	15.0 (d)	–22.6 (s)	4074	2679	18.1
(*trans*-$\mathbf{B_2}$)·$(\mathbf{C})_2$[c]	15.2 (br. s)	15.2 (br. s)	–24.1 (s)	4091	2652	–

[a] Spectra were measured in CD_3OD. [b] Multiplicities are given for the central lines. [c] The triplet and doublet resonances of P_X and P_Y coalesce as one broad central line.

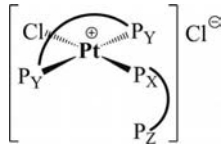

Figure 3. Phosphorus numbering in *trans*-$\mathbf{B_2}$.

Reaction of $[PtCl_2(MeCN)_2]$ with 1 equiv. of **A** in CD_3OD at 20 °C resulted in the disappearance of **A** and the formation of *cis*-$\mathbf{B_1}$ (79%) and *trans*-$\mathbf{B_2}$ (21%) after two hours (Scheme 3 and Figure 4, a). At 20 °C a slow transformation of *trans*-$\mathbf{B_2}$ to *cis*-$\mathbf{B_1}$ was observed; after three hours at 20 °C their ratio changed to *cis*-$\mathbf{B_1}$ (81%) and *trans*-$\mathbf{B_2}$ (19%). Upon heating the NMR tube to 60 °C, *trans*-$\mathbf{B_2}$ transformed immediately and quantitatively into *cis*-$\mathbf{B_1}$ (Scheme 3 and Figure 4, b).

Subsequently, we added an excess of ligand to the metal precursor in order study the effect on the product distribution. Reaction of $[PtCl_2(MeCN)_2]$ with 2 equiv. of **A** in CD_3OD at 20 °C resulted in the consumption of 53% of **A** and in the formation of a larger amount of *trans*-$\mathbf{B_2}$, i.e. *cis*-

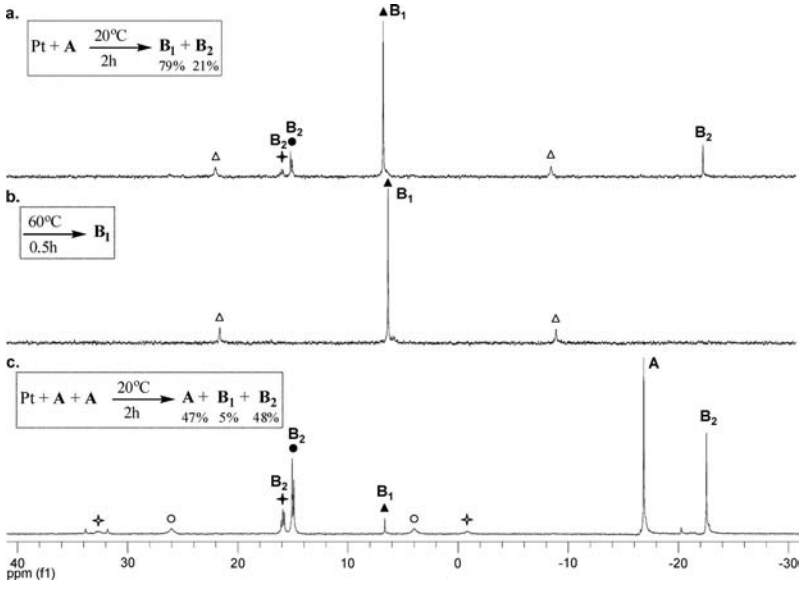

Figure 4. In situ $^{31}P\{^1H\}$ NMR experiments in CD_3OD of $[PtCl_2(MeCN)_2]$ and **A** to give *cis*-$\mathbf{B_1}$ and *trans*-$\mathbf{B_2}$.

B_1 (9%) and *trans*-**B_2** (91%) after two hours (Scheme 3 and Figure 4, c). A very slow transformation of *cis*-**B_1** to *trans*-**B_2** at 20 °C was observed; after one night at 20 °C their ratio changed to *cis*-**B_1** (7%) and *trans*-**B_2** (93%). Upon heating the NMR tube to 60 °C for five hours, a large amount of *trans*-**B_2** transformed into *cis*-**B_1**, i.e. *cis*-**B_1** (51%) and *trans*-**B_2** (49%), which was accompanied by an increase of the amount of **A** (Scheme 3).

In summary, upon reaction of **A** with the Pt precursor, *cis*-**B_1** is formed as the major product at lower and higher temperatures (20 °C and 60 °C), and *trans*-**B_2** is formed as the major product only when 2 equiv. of ligand are applied at lower temperatures (20 °C). These results imply that, under the given conditions, *cis*-**B_1** is the thermodynamic product and *trans*-**B_2** is the kinetic product (at a Pt/PP ratio of 1:1).

2. Platinum Capsules

Pt Capsules by Self-Assembly of Preformed Metal Complexes

Platinum encapsulation can be achieved by self-assembly of a platinum complex containing **A** and **C** or by the reaction between a platinum precursor and a diphosphane capsule. Self-assembly of the platinum capsules from preformed metal complexes was carried out by mixing methanol solutions of the precharged platinum complex (*cis*-**B_1** or *trans*-**B_2**) and the tetrasulfonatocalix[4]arene tetrasodium salt **C-SO_3Na** (Scheme 4). The platinum capsules (*cis*-**B_1**)·**C** and (*trans*-**B_2**)·(**C**)$_2$ formed instantaneously with NaOTs formed as a sideproduct. The platinum complexes *cis*-**B_1** and *trans*-**B_2** contain 1 and 2 equiv. of the tetracationic diphosphane ligand **A**, respectively. Hence, capsule (*cis*-**B_1**)·**C** contains one unit of **C**, whereas capsule (*trans*-**B_2**)·(**C**)$_2$ contains two.

The ESI-MS of (*cis*-**B_1**)·**C** and (*trans*-**B_2**)·(**C**)$_2$ confirmed their formation and stabilities in the gas phase (Figure 5, a,

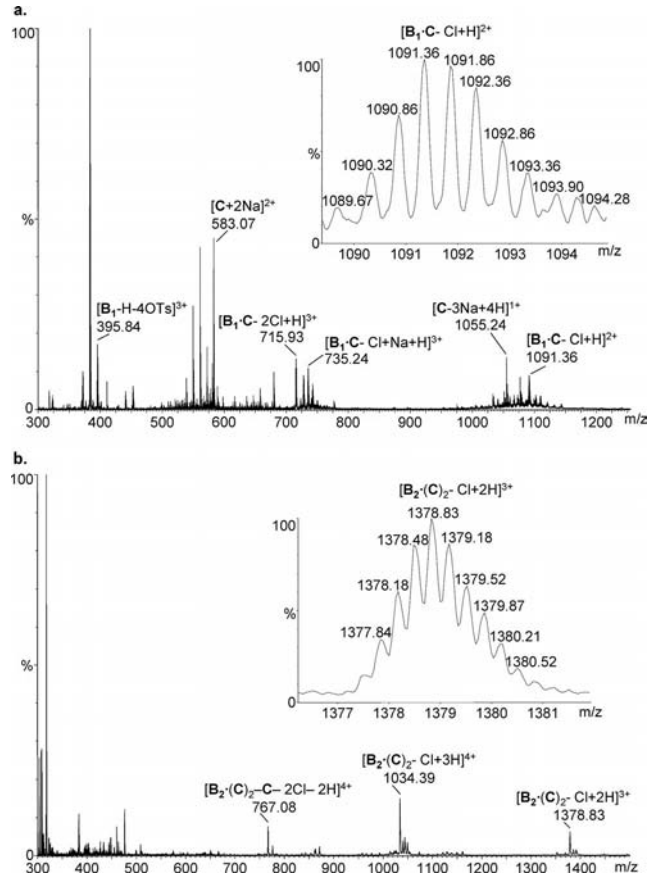

Figure 5. ESI-MS spectra of (*cis*-**B_1**)·**C** (*cis*-**B_1** + **C** → (*cis*-**B_1**)·**C**) (a) and (*trans*-**B_2**)·(**C**)$_2$ [Pt + **A**·**C** → (*trans*-**B_2**)·(**C**)$_2$] (b) in CH_3OH (inset: measured isotope patterns, see Supporting Information).

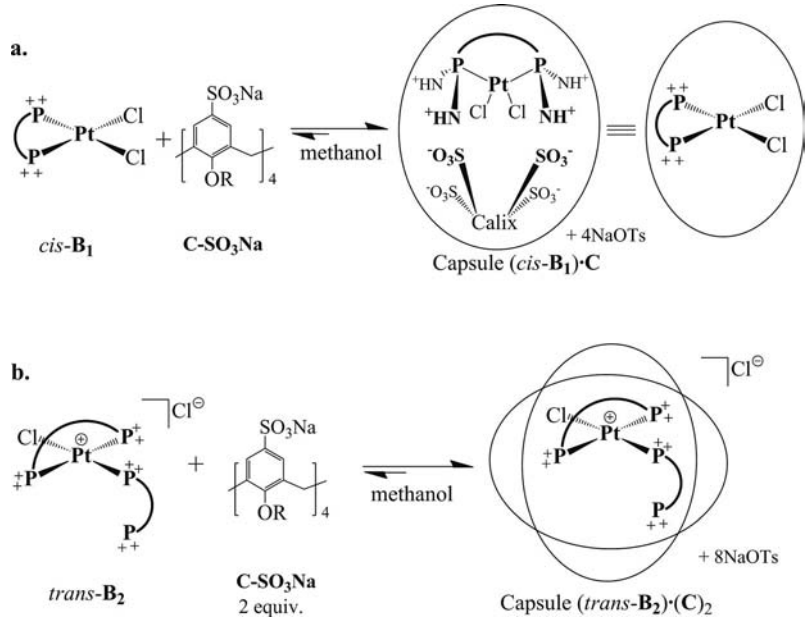

Scheme 4. Platinum encapsulation: self-assembly of (*cis*-**B_1**)·**C** (a) and (*trans*-**B_2**)·(**C**)$_2$ (b).

and Table 2, Entries 2 and 4). Prominent ion peaks were observed for the platinum capsules in CH_3OH. The charge on the capsules is created by loss of chloride ions from the platinum complex and/or by addition of protons or sodium cations from the solution. The ESI-MS of (*cis*-**B$_1$**)·**C** and (*trans*-**B$_2$**)·(**C**)$_2$ confirm that *cis*-**B$_1$** and *trans*-**B$_2$** remain intact upon capsule formation. (*cis*-**B$_1$**)·**C** and (*trans*-**B$_2$**)·(**C**)$_2$ gave very broad proton resonances in their ^{1}H NMR spectra and therefore could not be characterized by ^{1}H NMR spectroscopy.[5c,7]

Table 2. ESI-MS data[a,b] of *cis*-**B$_1$**, *trans*-**B$_2$**, (*cis*-**B$_1$**)·**C** and (*trans*-**B$_2$**)·(**C**)$_2$.

Entry	Compound (formation) [c]	Assignment [d] (Elemental composition)	Found *m/z*	Calcd. *m/z*
1	*cis*-**B$_1$**	[**B$_1$**-2OTs]$^{2+}$ ($C_{73}H_{94}Cl_2N_4O_7P_2PtS_2$)	765.25	765.25
2	(*cis*-**B$_1$**)·**C** (**B$_1$** + **C** →)	[**B$_1$**·**C** – Cl + H]$^{2+}$ ($C_{103}H_{133}ClN_4O_{21}P_2PtS_4$)	1091.36	1091.36
3	*trans*-**B$_2$**	[**B$_2$** – Cl – H– 3OTs]$^{3+}$ ($C_{153}H_{194}ClN_8O_{17}S_5P_4Pt$)	977.06	977.05
4	(*trans*-**B$_2$**)·(**C**)$_2$ (**B$_2$** + 2**C** →)	[**B$_2$**·(**C**)$_2$ – Cl + 2H + Na]$^{4+}$ ($C_{206}H_{266}ClN_8O_{42}P_4PtS_8Na$)	1039.87	1039.87
5	(*trans*-**B$_2$**)·(**C**)$_2$ (Pt + **A**·**C** →)	[**B$_2$**·(**C**)$_2$ – Cl + 2H]$^{3+}$ ($C_{206}H_{266}ClN_8O_{42}P_4PtS_8$)	1378.83	1378.83
6	(*trans*-**B$_2$**)·(**C**)$_2$ [e] (Pt + **A**·**C** →)	[**B$_2$**·(**C**)$_2$ – **C** – Cl – H]$^{4+}$ ($C_{162}H_{211}ClN_8O_{22}P_4PtS_4$)	776.07	776.07

[a] The ESI-MS were measured in CH_3OH. [b] See the Exp. Section and Supporting Information for more ion peaks and the measured and calculated isotope patterns. [c] The reaction equations given in the brackets describe the way the Pt capsules were formed. [d] OTs = $C_7H_7SO_3$. [e] The same ion peaks of (*trans*-**B$_2$**)·**C** were observed in the ESI-MS of (*trans*-**B$_2$**)·(**C**)$_2$ formed by self-assembly, i.e. *trans*-**B$_2$** + 2**C**.

Pt Capsules by Coordination to Preformed Ligand Capsule

Platinum encapsulation can also be achieved by the reaction of a platinum precursor and the preformed diphosphane capsule **A**·**C**. The ionic-based diphosphane capsule **A**·**C** consists of the tetracationic diphosphane **A** and **C** (Scheme 5).[5b–5c] Mixing methanol solutions of the neutral building blocks **a** and **C-SO$_3$H** resulted in quantitative protonation of **a** by **C-SO$_3$H**, which led to capsule **A**·**C** without salt formation.[11]

Depending on the conditions used, reaction of [$PtCl_2$(MeCN)$_2$] with **A**·**C** in methanol led to the formation of the platinum capsules (*cis*-**B$_1$**)·**C** and (*trans*-**B$_2$**)·(**C**)$_2$, vide infra, as indicated by in situ ^{31}P{^{1}H} NMR spectroscopy and ESI-MS (Scheme 6, Figure 5, b and Table 2, Entry 5). The chemical shifts of the Pt capsules in the ^{31}P{^{1}H} NMR spectra are comparable to those of their corresponding Pt complexes but the signals of the capsules are broad.[5c] The phosphorus resonances of (*cis*-**B$_1$**)·**C** show a characteristic 1/4/1 pattern consisting of a singlet at 6.6 ppm, flanked by ^{195}Pt satellites with a coupling constant $J_{Pt–P}$ of 3727 Hz (Table 1 and Figure 6, b). The ^{31}P{^{1}H} NMR spectrum of (*trans*-**B$_2$**)·(**C**)$_2$ consists of one singlet at –24.1 ppm (1 P) assigned to the noncoordinating P_Z, and one singlet at 15.2 ppm (3 P) assigned to P_X and P_Y (Table 1 and Figure 6, a). As a result of signal broadening, the resonances of P_X and P_Y coalesce into one broad singlet. Still, the Pt satellites of (*trans*-**B$_2$**)·(**C**)$_2$ are visible (P_X: $J_{P–Pt}$ = 4091 Hz and P_Y: $J_{P–Pt}$ = 2652 Hz) confirming that *trans*-**B$_2$** has the same structure in its encapsulated form.

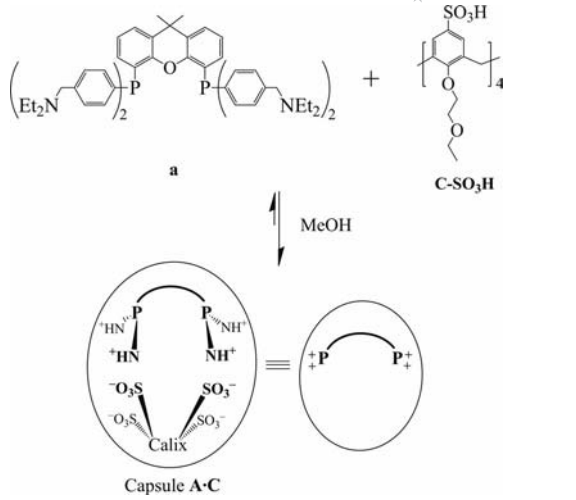

Scheme 5. Self-assembly of **A**·**C** from neutral building blocks.

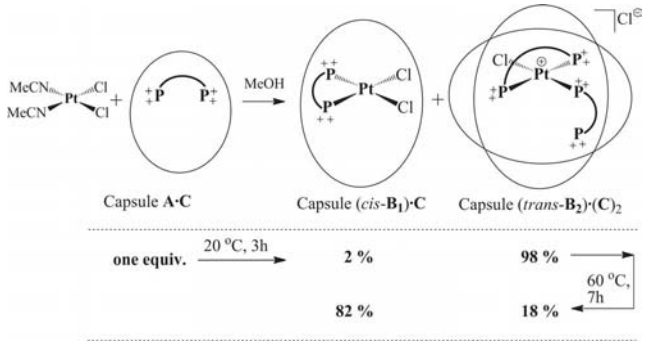

Scheme 6. Platinum encapsulation by reaction of [$PtCl_2$(MeCN)$_2$] with **A**·**C** to give (*cis*-**B$_1$**)·**C** and (*trans*-**B$_2$**)·(**C**)$_2$.

The ESI-MS of (*trans*-**B$_2$**)·(**C**)$_2$ formed by the reaction of [$PtCl_2$(MeCN)$_2$] with **A**·**C** supports the presence of two **C** units around *trans*-**B$_2$** (Figure 5, b and Table 2, Entry 5). Interestingly, in the ESI-MS of (*trans*-**B$_2$**)·(**C**)$_2$ we also observed ion peaks corresponding to [**B$_2$**·**C**]$^{4+}$, i.e. [**B$_2$**·(**C**)$_2$ – **C** – Cl – H]$^{4+}$ (Figure 5, b and Table 2, Entry 6). We assume that [**B$_2$**·**C**]$^{4+}$ is formed by abstraction of one **C** unit from (*trans*-**B$_2$**)·(**C**)$_2$ during the ionization process.

Reaction of [$PtCl_2$(MeCN)$_2$] with 1 equiv. of **A**·**C** in methanol at 20 °C resulted in the disappearance of **A**·**C** and the formation of (*cis*-**B$_1$**)·**C** (2%) and (*trans*-**B$_2$**)·(**C**)$_2$ (98%) after three hours (Scheme 6 and Figure 6, a). We observed a slow transformation of (*trans*-**B$_2$**)·(**C**)$_2$ to (*cis*-**B$_1$**)·**C** at 20 °C; after one night at 20 °C their ratio changed to (*cis*-**B$_1$**)·**C** (9%) and (*trans*-**B$_2$**)·(**C**)$_2$ (91%). Upon heating the NMR tube to 60 °C, (*trans*-**B$_2$**)·(**C**)$_2$ continued to transform into (*cis*-**B$_1$**)·**C** up to (*cis*-**B$_1$**)·**C** (82%) and (*trans*-**B$_2$**)·(**C**)$_2$ (18%) (Scheme 6 and Figure 6, b). This ratio was reached after seven hours at 60 °C and did not change even after eight more hours.

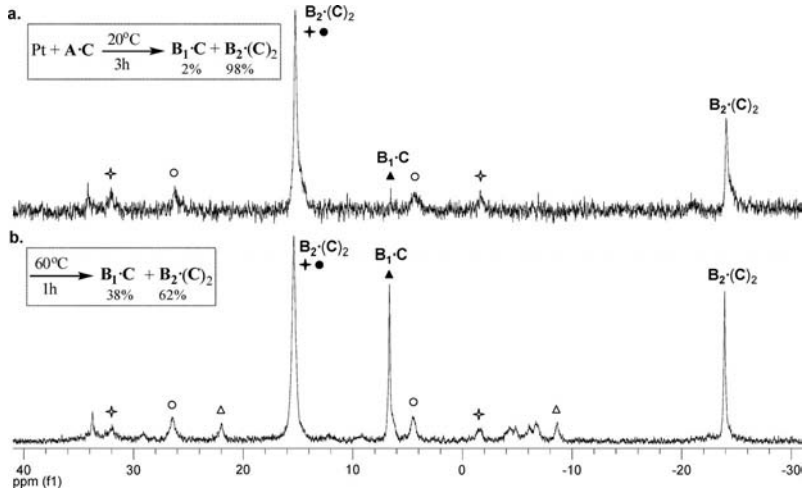

Figure 6. In situ $^{31}P\{^{1}H\}$ NMR experiments in CD_3OD of $[PtCl_2(MeCN)_2]$ and **A·C** to give (*cis*-**B$_1$**)·**C** and (*trans*-**B$_2$**)·(**C**)$_2$ at 20 °C (a) and at 60 °C (b).

In summary, at lower temperatures (20 °C) the reaction of $[PtCl_2(MeCN)_2]$ with **A·C** results in (*trans*-**B$_2$**)·(**C**)$_2$ as the major product (98%), whereas the same reaction with **A** results in *cis*-**B$_1$** as the major product (79%). At higher temperatures (60 °C) both **A·C** and **A** have a preference towards the *cis* species, i.e. (*cis*-**B$_1$**)·**C** (82%) and *cis*-**B$_1$** (100%), respectively. The difference in product selectivity between **A·C** and **A** at low temperatures shows that the presence of two calix[4]arenes around the platinum complex stabilizes the kinetic product, i.e. the *trans*-**B$_2$** species. This stabilization is supported by the incomplete transformation to the *cis*-Pt complex (82%) at high temperatures.

3. Molecular Modelling Study

The modelled structures of the platinum complexes *cis*-**B$_1$** and *trans*-**B$_2$** were first calculated using DFT, and the optimized structures were subsequently used as input for PM3 calculations. In order to calculate the structures of capsules (*cis*-**B$_1$**)·**C** and (*trans*-**B$_2$**)·(**C**)$_2$, the structures of *cis*-**B$_1$** and *trans*-**B$_2$** were frozen, except for the diethylammoniummethyl substituents, and **C** molecules were added (modelled at the PM3 level). These structures were used as input for molecular mechanics calculations (MMFF), and subsequently the structure of (*cis*-**B$_1$**)·**C** was also subjected to PM3 calculation [PM3 calculation of (*trans*-**B$_2$**)·(**C**)$_2$ failed because it is too large]. The modelled structure of *cis*-**B$_1$** (with a xantphos ligand) illustrates the square planar geometry around platinum. The modelled structure of capsule (*cis*-**B$_1$**)·**C** illustrates that *cis*-**B$_1$** and **C** are complementary, facing one another, as a result of interaction between the ammonium and sulfonato groups. In addition, the platinum ion is located inside the capsule (Figure 7, a).

The modelled structure of the bisligated complex *trans*-**B$_2$** (with two xantphos ligands) shows that the ionic Pt complex adopts a distorted square planar geometry with the first diphosphane ligand coordinating to platinum in a *trans* fashion and the second in a monodentate fashion (Figure 7, b). The monodentate ligand is situated partly between the two $P(Ar)_2$ groups of the bidentate ligand. Consequently, **C** cannot interact solely with the bidentate ligand or solely with the monodentate ligand. The modelled structure of (*trans*-**B$_2$**)·(**C**)$_2$ illustrates that two molecules of the rigid, concave calix[4]arene interact with *trans*-**B$_2$** (Figure 7, c). One of the two tetraanionic calix[4]arenes interacts with four cationic groups of *trans*-**B$_2$** bound to four different phosphorus atoms and the other calix[4]arene interacts with three cationic groups of *trans*-**B$_2$** situated at three different phosphorus atoms. Hence, each calix[4]arene interacts simultaneously with both ligands. Consequently, (*trans*-**B$_2$**)·

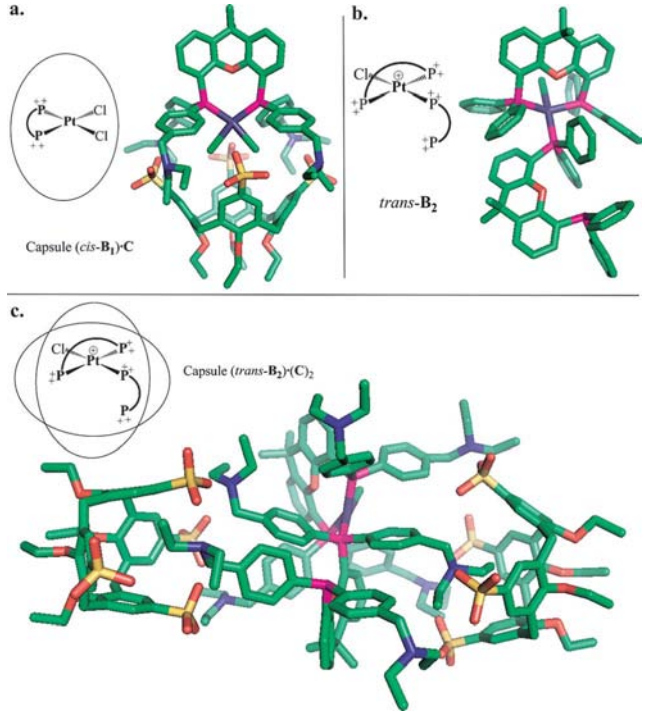

Figure 7. Modelled structures and schematic pictures of (*cis*-**B$_1$**)·**C** (a), *trans*-**B$_2$** (with xantphos ligands) (b) and (*trans*-**B$_2$**)·(**C**)$_2$ (c).

EurJIC European Journal of Inorganic Chemistry

$(\mathbf{C})_2$ is composed of two semicapsules with an undefined structure. The platinum atom is situated between (not within) the two semicapsules, i.e. the platinum atom is not directly encapsulated. Interestingly, (*trans*-$\mathbf{B_2}$)·$(\mathbf{C})_2$ has a sandwich-like structure with the two calix[4]arenes pointing towards one another and the platinum complex is situated in between. The modelled structure of (*trans*-$\mathbf{B_2}$)·$(\mathbf{C})_2$ displays only one of the possible conformations and therefore it is likely that the two calix[4]arenes interact with *trans*-$\mathbf{B_2}$ in more ways than we have presented here.

Kinetic Product Stabilization

We know that upon reaction of $[PtCl_2(MeCN)_2]$ with **A** or **A**·**C**, the kinetic products *trans*-$\mathbf{B_2}$ and (*trans*-$\mathbf{B_2}$)·$(\mathbf{C})_2$ are the first products that are formed. Subsequently, upon coordination of the Pt precursor to the noncoordinating phosphorus atom of *trans*-$\mathbf{B_2}$, the kinetic products transform into the thermodynamic products *cis*-$\mathbf{B_1}$ and (*cis*-$\mathbf{B_1}$)·**C**, respectively. The low solubility of $[PtCl_2(MeCN)_2]$ in methanol results initially in an excess of **A** and **A**·**C** with respect to the metal, which enhances the formation of the kinetic product (as observed by in situ $^{31}P\{^1H\}$ NMR). The kinetic product, (*trans*-$\mathbf{B_2}$)·$(\mathbf{C})_2$, is stabilized by the two calix[4]arene units, and therefore the formation of the corresponding thermodynamic product, (*cis*-$\mathbf{B_1}$)·**C**, is inhibited [at 20 °C, Pt/PP = 1, (*cis*-$\mathbf{B_1}$)·**C** 2% and (*trans*-$\mathbf{B_2}$)·$(\mathbf{C})_2$ 98%]. In contrast, the kinetic product *trans*-$\mathbf{B_2}$ is not stabilized by its eight tosylate counterions and therefore it transforms immediately to the corresponding thermodynamic product *cis*-$\mathbf{B_1}$ (at 20 °C, Pt/PP = 1, *cis*-$\mathbf{B_1}$ 79% and *trans*-$\mathbf{B_2}$ 21%). Steric congestion is created around *trans*-$\mathbf{B_2}$ in (*trans*-$\mathbf{B_2}$)·$(\mathbf{C})_2$ by the two calix[4]arenes. This inhibits the access of the Pt precursor to the noncoordinating phosphorus atom of *trans*-$\mathbf{B_2}$ and consequently the formation of the thermodynamic product, (*cis*-$\mathbf{B_1}$)·**C**, is also inhibited. The modelled structure of (*trans*-$\mathbf{B_2}$)·$(\mathbf{C})_2$ implies that each tetraanionic calix[4]arene interacts with the cationic groups of the two different ligands of *trans*-$\mathbf{B_2}$ and consequently fix the spatial orientation of the two ligands relative to each other, which results in the stabilization of the kinetic product. This stabilization of (*trans*-$\mathbf{B_2}$)·$(\mathbf{C})_2$ compared to *trans*-$\mathbf{B_2}$, leads to a higher energy barrier for transformation of the kinetic product, (*trans*-$\mathbf{B_2}$)·$(\mathbf{C})_2$, into the thermodynamic product, (*cis*-$\mathbf{B_1}$)·**C** and a relative shift in equilibrium to the *trans*-Pt species.

Conclusions

We have demonstrated that the coordination geometry around a platinum atom can be influenced by supramolecular capsules. The capsule used in this study is formed by ionic interactions and is composed of a tetracationic xantphos-type diphosphane ligand and a complementary tetraanionic calix[4]arene. Reaction of the diphosphane capsule with a platinum precursor yields the bisligated biscalix[4]arene *trans*-Pt capsule, whereas the same diphosphane in the absence of calix[4]arene prefers the formation of the monoligated *cis*-Pt complex, indicated by $^{31}P\{^1H\}$ NMR and ESI-MS. The two calix[4]arenes stabilize the kinetic product, the *trans*-Pt species, and slow the formation of the thermodynamic product, the *cis*-Pt species. This new supramolecular strategy for controlling the coordination chemistry of transition metal complexes reveals new opportunities to control the activity, stability and selectivity of the potential homogeneous catalysts.

Experimental Section

General Remarks: All reactions were carried out under a dry, inert atmosphere of purified nitrogen or argon using standard Schlenk techniques, unless stated otherwise. Solvents were dried and distilled under nitrogen prior to use. Diethyl ether was distilled with sodium/benzophenone. Methanol was distilled with CaH_2. Deuterated solvents were distilled with the appropriate drying agents. Unless stated otherwise, all chemicals were obtained from commercial suppliers and used as received. 4,5-Bis(bis{*p*-[(diethylamino)-methyl]phenyl}phosphanyl)-9,9-dimethylxanthene (**a**),[5b] 4,5-bis-(bis{*p*-[(diethylammonium tosylate)methyl]phenyl}phosphanyl)-9,9-dimethylxanthene **A-HOTs** (**A**),[5d] 5,11,17,23-tetrakis(sulfonato)-25,26,27,28-tetrakis(2-ethoxyethoxy)calix[4]arene tetrasodium salt (**C-SO$_3$Na**)[5b,12] and 25,26,27,28-tetrakis(2-ethoxyethoxy)calix[4]arene-5,11,17,23-tetrasulfonic acid (**C-SO$_3$H**)[5c] were synthesized according to reported procedures. NMR spectra were recorded with Varian Inova 500, Bruker Avance DRX 300 and Varian Mercury 300 NMR spectrometers. Chemical shifts are given in ppm relative to TMS (^1H and ^{13}C NMR) and 85% H_3PO_4 ($^{31}P\{^1H\}$ NMR). HRMS (FAB) measurements were carried out with a JEOL JMS SX/SX 102A at the Department of Mass Spectrometry at the University of Amsterdam. ESI-MS measurements were carried out with a Q-TOF (Micromass, Waters, Whyttenshawe, UK) mass spectrometer equipped with a Z-spray orthogonal nanoelectrospray source, using Econo Tips (New Objective, Woburn, MA) to create an off line nanospray, at the Department of Mass Spectrometry of Biomacromolecules at the University of Amsterdam. The MS spectra were processed with software tools embedded in Masslynx software (Micromass, Waters, Whyttenshawe, UK), additional isotopic pattern analysis was performed with the use of the Bruker Daltonics Isotope Pattern software program (Bruker Daltonik, Bremen, Germany, version 1.0.125.0), and the calculated isotope patterns shown in the Supporting Information were calculated using the IsoPro 3.1 software program. Molecular modelling calculations were performed using Spartan ′08 V1.0.3 software (B3LYP LACVP basis set).

***cis*-[Pt(A)Cl$_2$] (*cis*-$\mathbf{B_1}$): A-HOTs** (97.4 mg, 60.57 μmol) was added to a fine suspension of $[PtCl_2(MeCN)_2]$ (21.08 mg, 60.57 μmol) in methanol (8 mL). After stirring for 1 h at room temperature, the clear reaction mixture was heated to reflux overnight. The solvent was evaporated, and the yellow solid was washed three times with diethyl ether. *cis*-$\mathbf{B_1}$ was obtained as a pale yellow microcrystalline powder. $^{31}P\{^1H\}$ NMR (121.5 MHz, CD_3OD, 293 K): δ = 6.2 (s, J_{Pt-P} = 3728 Hz) ppm. ^1H NMR (300 MHz, CD_3OD, 293 K): δ = 7.87 (d, J = 7.5 Hz, 2 H), 7.70 (d, J = 8.1 Hz, 8 H, OTs^-), 7.61–7.14 (m, 20 H), 7.25 (d, J = 8.4 Hz, 8 H, OTs^-), 4.31 (s, 8 H, CH_2N), 3.04 (m, 16 H, NCH_2CH_3), 2.34 (s, 12 H, OTs^-), 1.87 [s, 6 H, $C(CH_3)_2$], 1.22 (t, J = 7.8 Hz, 24 H, NCH_2CH_3) ppm. *cis*-$\mathbf{B_1}$ gave broad carbon resonances in its $^{13}C\{^1H\}$ NMR spectrum and therefore could not be characterized by ^{13}C NMR spectroscopy.

Self-Assembly of A·C: A methanol solution of **C-SO_3H** (1 equiv.) was slowly added to a methanol solution of **a** (1 equiv.). The solution was stirred for 30 min at room temperature before the solvent was evaporated, which left **A·C**. Observed upfield shifts of the proton resonances ($\Delta\delta_H$) of the $CH_2NH^+(CH_2CH_3)_2$ protons of **A·C**, with respect to those of the corresponding free **A-HOTs** in CD_3OD: $\Delta\delta(CH_2CH_3)$ = 0.37, $\Delta\delta(CH_2CH_3)$ = 0.34 and $\Delta\delta(NCH_2)$ = 0.25 ppm (**A**/**C** = 1:1). ESI-MS (CH_3OH): *m*/*z* = 977.06 [**A·C** + 2H]$^{2+}$, 651.74 [**A·C** + 3H]$^{3+}$.

Self-Assembly of (*cis*-B_1)·C: Equimolar methanol solutions of *cis*-B_1 and **C-SO_3Na** were mixed at room temperature, which resulted in the immediate formation of (*cis*-B_1)·**C** together with 4 equiv. of NaOTs.

Self-Assembly of (*trans*-B_2)·$(C)_2$: Methanol solutions of *trans*-B_2 (synthesized in situ) (1 equiv.) and **C-SO_3Na** (2 equiv.) were mixed at room temperature, which resulted in the immediate formation of (*trans*-B_2)·$(C)_2$ together with 8 equiv. of NaOTs.

In situ VT $^{31}P\{^1H\}$ NMR Studies

***cis*-B_1:** A solution of $[PtCl_2(MeCN)_2]$ (2.611 mg, 7.5 μmol, 1 equiv.) and **A-HOTs** (12.060 mg, 7.5 μmol, 1 equiv.) in CD_3OD (0.5 mL) was vigorously stirred for 2 h at room temperature to ensure that all the reactants dissolved. The reaction mixture was transferred into a NMR tube and the reaction was followed by $^{31}P\{^1H\}$ NMR over time, i.e. 3 h at 20 °C and 3 h at 60 °C.

***trans*-B_2:** A solution of $[PtCl_2(MeCN)_2]$ (2.611 mg, 7.5 μmol, 1 equiv.) and **A-HOTs** (24.120 mg, 15.0 μmol, 2 equiv.) in CD_3OD (0.5 mL) was vigorously stirred for 2 h at room temperature to ensure that all the reactants dissolved. The reaction mixture was transferred into a NMR tube and the reaction was followed by $^{31}P\{^1H\}$ NMR over time, i.e. 16 h at 20 °C and 5 h at 60 °C. (*cis*-B_1)·**C and** (*trans*-B_2)·$(C)_2$**:** A solution of $[PtCl_2(MeCN)_2]$ (2.611 mg, 7.5 μmol, 1 equiv.) and **A·C** (14.643 mg, 7.5 μmol, 1 equiv.) in CD_3OD (0.5 mL) was vigorously stirred for 3 h at room temperature to ensure that all the reactants dissolved. The reaction mixture was transferred into a NMR tube and the reaction was followed by $^{31}P\{^1H\}$ NMR over time, i.e. 16 h at 20 °C and 20 h at 60 °C.

ESI-MS: Samples of the complexes and capsules with initial concentrations of 100–250 μM were diluted in MeOH to a final concentration of 1%. ESI-MS analysis of *cis*-B_1 was carried out with an isolated sample of *cis*-B_1. ESI-MS analysis of *trans*-B_2 was carried out with an in situ generated sample of *trans*-B_2, which was prepared by stirring a methanol solution of $[PtCl_2(MeCN)_2]$ and **A** (2 equiv.) overnight at 20 °C. ESI-MS analysis of (*cis*-B_1)·**C** was carried out by mixing methanol solutions of *cis*-B_1 and **C**, i.e. self-assembly. ESI-MS analysis of (*trans*-B_2)·$(C)_2$ was performed in two ways: (1) by mixing methanol solutions of *trans*-B_2 and **C**, i.e. self-assembly and (2) by using an in situ generated sample of (*trans*-B_2)·$(C)_2$, which was prepared by stirring a methanol solution of $[PtCl_2(MeCN)_2]$ and **A·C** overnight at 20 °C. No ion peaks for higher aggregates than 1:1 for (*cis*-B_1)·**C** and 1:2 for (*trans*-B_2)·$(C)_2$ were detected. Comparison of the measured isotope patterns of the Pt complexes and capsules with those calculated confirms the elemental composition and charge state (see Supporting Information). The reported *m*/*z* values correspond to the 100% ion peak (isotope with the highest intensity).

cis-B_1: ESI-MS (CH_3OH): *m*/*z* = 765.25 [B_1 – 2OTs]$^{2+}$, 661.26 [B_1 – Cl – 2H – 3OTs]$^{2+}$, 575.25 [B_1 – Cl – 3H – 4OTs]$^{2+}$, 453.17 [B_1-3OTs]$^{3+}$, 441.18 [B_1 – Cl – H – 3OTs]$^{3+}$, 395.84 [B_1 – H – 4OTs]$^{3+}$, 383.82 [B_1 – Cl – 2H – 4OTs]$^{3+}$.

trans-B_2: ESI-MS (CH_3OH): *m*/*z* = 977.06 [B_2 – Cl – H – 3OTs]$^{3+}$, 919.71 [B_2 – Cl – 2H – 4OTs]$^{3+}$, 862.37 [B_2 – Cl –3H – 5OTs]$^{3+}$, 805.04 [B_2 – Cl – 4H – 6OTs]$^{3+}$, 690.03 [B_2 – Cl – H – 4OTs]$^{4+}$, 594.79 [B_2-2Cl – 4H – 6OTs]$^{4+}$.

(*cis*-B_1)·**C**: ESI-MS (CH_3OH): *m*/*z* = 1109.86 [B_1·**C** + 2H]$^{2+}$, 1091.36 [B_1·**C** – Cl + H]$^{2+}$, 715.93 [B_1·**C** – 2Cl + H]$^{3+}$, 723.23 [B_1·**C** – 2Cl + Na]$^{3+}$, 727.91 [B_1·**C** – Cl + 2H]$^{3+}$, 735.24 [B_1·**C** – Cl + Na + H]$^{3+}$, 742.55 [B_1·**C** – Cl + 2Na]$^{3+}$.

Self-assembly of (*trans*-B_2)·$(C)_2$ from *trans*-B_2 **+ C**: ESI-MS (CH_3OH): *m*/*z* = 1393.48 [B_2·$(C)_2$ – Cl + 2Na]$^{3+}$, 1378.83 [B_2·$(C)_2$ – Cl + 2H]$^{3+}$, 1034.39 [B_2·$(C)_2$ – Cl + 3H]$^{4+}$, 1039.87 [B_2·$(C)_2$ – Cl + 2H + Na]$^{4+}$, 1045.35 [B_2·$(C)_2$ – Cl + H + 2Na]$^{4+}$, 1050.86 [B_2·$(C)_2$ – Cl + 3Na]$^{4+}$, 776.07 [B_2·$(C)_2$ – **C** – Cl – H]$^{4+}$, 767.08 [B_2·$(C)_2$ – **C** – 2Cl – 2H]$^{4+}$.

Reaction of $[PtCl_2(MeCN)_2]$ and **A·C** to give (*trans*-B_2)·$(C)_2$: ESI-MS (CH_3OH): *m*/*z* = 1378.83 [B_2·$(C)_2$ – Cl + 2H]$^{3+}$, 1034.39 [B_2·$(C)_2$ – Cl + 3H]$^{4+}$, 767.08 [B_2·$(C)_2$ – **C** – 2Cl – 2H]$^{4+}$, 776.07 [B_2·$(C)_2$ – **C** – Cl – H]$^{4+}$.

Supporting Information (see footnote on the first page of this article): ESI-MS, measured and calculated isotope patterns of the compounds.

[1] a) P. W. N. M. Van Leeuwen (Ed.), *Supramolecular catalysis*, Wiley-VCH, Weinheim, Germany, **2008**; b) T. S. Koblenz, J. Wassenaar, J. N. H. Reek, *Chem. Soc. Rev.* **2008**, *37*, 247–262; c) J. I. Van der Vlugt, T. S. Koblenz, J. Wassenaar, J. N. H. Reek, *Chemistry in Self-Assembled Nanoreactors*, in: *Molecular Encapsulation: Organic Reactions in Constrained Systems* (Eds.: U. H. Brinker, J.-L. Mieusset), p. 145–174, John Wiley & Sons, Chichester, UK, **2010**; d) D. M. Vriezema, M. C. Aragones, J. A. A. W. Elemans, J. J. L. M. Cornelissen, A. E. Rowan, R. J. M. Nolte, *Chem. Rev.* **2005**, *105*, 1445–1489; e) D. Fiedler, D. H. Leung, R. G. Bergman, K. N. Raymond, *Acc. Chem. Res.* **2005**, *38*, 349–358; f) D. H. Leung, R. G. Bergman, K. N. Raymond, *J. Am. Chem. Soc.* **2006**, *128*, 9781–9797; g) D. H. Leung, R. G. Bergman, K. N. Raymond, *J. Am. Chem. Soc.* **2007**, *129*, 2746–2747.

[2] a) V. F. Slagt, J. N. H. Reek, P. C. J. Kamer, P. W. N. M. van Leeuwen, *Angew. Chem.* **2001**, *113*, 4401; *Angew. Chem. Int. Ed.* **2001**, *40*, 4271–4274; b) V. F. Slagt, P. W. N. M. van Leeuwen, J. N. H. Reek, *Angew. Chem.* **2003**, *115*, 5777; *Angew. Chem. Int. Ed.* **2003**, *42*, 5619–5623; c) V. F. Slagt, P. C. J. Kamer, P. W. N. M. van Leeuwen, J. N. H. Reek, *J. Am. Chem. Soc.* **2004**, *126*, 1526–1536; d) A. W. Kleij, M. Lutz, A. L. Spek, P. W. N. M. van Leeuwen, J. N. H. Reek, *Chem. Commun.* **2005**, *29*, 3661–3663; e) A. W. Kleij, J. N. H. Reek, *Chem. Eur. J.* **2006**, *12*, 4218–4227; f) A. W. Kleij, M. Kuil, D. M. Tooke, A. L. Spek, J. N. H. Reek, *Inorg. Chem.* **2005**, *44*, 7696–7698; g) M. Kuil, T. Soltner, P. W. N. M. van Leeuwen, J. N. H. Reek, *J. Am. Chem. Soc.* **2006**, *128*, 11344–11345; h) J. Flapper, J. N. H. Reek, *Angew. Chem.* **2007**, *119*, 8744; *Angew. Chem. Int. Ed.* **2007**, *46*, 8590–8592.

[3] a) M. J. Wilkinson, P. W. N. M. van Leeuwen, J. N. H. Reek, *Org. Biomol. Chem.* **2005**, *3*, 2371–2383; b) M. Kuil, P. E. Goudriaan, A. W. Kleij, D. M. Tooke, A. L. Spek, P. W. N. M. van Leeuwen, J. N. H. Reek, *Dalton Trans.* **2007**, *22*, 2311–2320; c) P. E. Goudriaan, M. Kuil, X.-B. Jiang, P. W. N. M. van Leeuwen, J. N. H. Reek, *Dalton Trans.* **2009**, *10*, 1801–1805; d) L. K. Knight, Z. Freixa, P. W. N. M. van Leeuwen, J. N. H. Reek, *Organometallics* **2006**, *25*, 954–960; e) A. J. Sandee, A. M. van der Burg, J. N. H. Reek, *Chem. Commun.* **2007**, *8*, 864–866; f) D. Rivillo, H. Gulyas, J. Benet-Buchholz, E. C. Escudero-Adan, Z. Freixa, P. W. N. M. van Leeuwen, *Angew. Chem.* **2007**, *119*, 7385; *Angew. Chem. Int. Ed.* **2007**, *46*, 7247–7250; g) H. Gulyas, J. Benet-Buchholz, E. C. Escudero-Adan, Z. Freixa, P. W. N. M. van Leeuwen, *Chem. Eur. J.* **2007**, *13*, 3424–3430; h) B. Breit, *Angew. Chem.* **2005**, *117*, 6976; *Angew. Chem. Int. Ed.* **2005**, *44*, 6816–6825; i) W. Seiche, B. Breit,

Phosphorus Ligands Asymmetric Catal. **2008**, *2*, 848–885; j) S. A. Moteki, J. M. Takacs, *Angew. Chem.* **2008**, *120*, 908; *Angew. Chem. Int. Ed.* **2008**, *47*, 894–897.

[4] a) M. Fujita, K. Umemoto, M. Yoshizawa, N. Fujita, T. Kusukawa, K. Biradha, *Chem. Commun.* **2001**, *6*, 509–518; b) J. Rebek Jr., *Angew. Chem.* **2005**, *117*, 2104; *Angew. Chem. Int. Ed.* **2005**, *44*, 2068–2078; c) F. Hof, S. L. Craig, C. Nuckolls, J. Rebek Jr., *Angew. Chem.* **2002**, *114*, 1556; *Angew. Chem. Int. Ed.* **2002**, *41*, 1488–1508; d) M. M. Conn, J. Rebek Jr, *Chem. Rev.* **1997**, *97*, 1647–1668.

[5] a) T. S. Koblenz, H. L. Dekker, C. G. De Koster, P. W. N. M. van Leeuwen, J. N. H. Reek, *Chem. Commun.* **2006**, *16*, 1700–1702; b) T. S. Koblenz, H. L. Dekker, C. G. De Koster, P. W. N. M. van Leeuwen, J. N. H. Reek, *Chem. Asian J.* **2011**, *6*, 2431; c) T. S. Koblenz, H. L. Dekker, C. G. De Koster, P. W. N. M. van Leeuwen, J. N. H. Reek, *Chem. Asian J.* **2011**, *6*, 2444; d) T. S. Koblenz, M. Kuil, V. Bocokic, P. W. N. M. van Leeuwen, J. N. H. Reek, manuscript in preparation.

[6] a) M. Kranenburg, Y. E. M. van der Burgt, P. C. J. Kamer, P. W. N. M. van Leeuwen, K. Goubitz, J. Fraanje, *Organometallics* **1995**, *14*, 3081–3089; b) P. W. N. M. van Leeuwen, P. C. J. Kamer, J. N. H. Reek, *Pure Appl. Chem.* **1999**, *71*, 1443–1452; c) P. W. N. M. Van Leeuwen, P. C. J. Kamer, J. N. H. Reek, P. Dierkes, *Chem. Rev.* **2000**, *100*, 2741–2769; d) P. C. J. Kamer, P. W. N. M. van Leeuwen, J. N. H. Reek, *Acc. Chem. Res.* **2001**, *34*, 895–904; e) Z. Freixa, P. W. N. M. van Leeuwen, *Dalton Trans.* **2003**, *10*, 1890–1901; f) M. A. Zuideveld, B. H. G. Swennenhuis, M. D. K. Boele, Y. Guari, G. P. F. van Strijdonck, J. N. H. Reek, P. C. J. Kamer, K. Goubitz, J. Fraanje, M. Lutz, A. L. Spek, P. W. N. M. van Leeuwen, *J. Chem. Soc., Dalton Trans.* **2002**, *11*, 2308–2317; g) J. Yin, S. L. Buchwald, *J. Am. Chem. Soc.* **2002**, *124*, 6043–6048; h) L. A. Van der Veen, P. K. Keeven, P. C. J. Kamer, P. W. N. M. van Leeuwen, *J. Chem. Soc., Dalton Trans.* **2000**, *13*, 2105–2112; i) M. Kranenburg, P. C. J. Kamer, P. W. N. M. van Leeuwen, *Eur. J. Inorg. Chem.* **1998**, *2*, 155–157; j) R. J. Van Haaren, K. Goubitz, J. Fraanje, G. P. F. van Strijdonck, H. Oevering, B. Coussens, J. N. H. Reek, P. C. J. Kamer, P. W. N. M. van Leeuwen, *Inorg. Chem.* **2001**, *40*, 3363–3372.

[7] G. Petocz, Z. Berente, T. Kegl, L. Kollar, *J. Organomet. Chem.* **2004**, *689*, 1188–1193.

[8] R. Van Duren, J. I. van der Vlugt, H. Kooijman, A. L. Spek, D. Vogt, *Dalton Trans.* **2007**, *10*, 1053–1059.

[9] a) Z. Freixa, M. S. Beentjes, G. D. Batema, C. B. Dieleman, G. P. F. van Strijdonck, J. N. H. Reek, P. C. J. Kamer, J. Fraanje, K. Goubitz, P. W. N. M. van Leeuwen, *Angew. Chem.* **2003**, *115*, 1322; *Angew. Chem. Int. Ed.* **2003**, *42*, 1284–1287; b) L. Poorters, D. Armspach, D. Matt, L. Toupet, S. Choua, P. Turek, *Chem. Eur. J.* **2007**, *13*, 9448–9461; c) R. Den Heeten, PhD Thesis, University of Amsterdam, The Netherlands, **2009**; d) Z. Freixa, P. W. N. M. van Leeuwen, *Coord. Chem. Rev.* **2008**, *252*, 1755–1786.

[10] L. Kollar, G. Szalontai, *J. Organomet. Chem.* **1991**, *421*, 341–345.

[11] a) R. Zadmard, T. Schrader, T. Grawe, A. Kraft, *Org. Lett.* **2002**, *4*, 1687–1690; b) B. Kuberski, A. Szumna, *Chem. Commun.* **2009**, *15*, 1959–1961.

[12] R. Fiammengo, P. Timmerman, J. Huskens, K. Versluis, A. J. R. Heck, D. N. Reinhoudt, *Tetrahedron* **2002**, *58*, 757–764.

Received: August 1, 2011
Published Online: September 16, 2011

